Large angle cosmic microwave background fluctuations from cosmic strings with a cosmological constant

M. Landriau*

Laboratoire de l'Accélérateur Linéaire, IN2P3-CNRS et Université Paris-Sud, Boîte Postale 34, 91898 Orsay Cedex, France

E. P. S. Shellard[†]

Department of Applied Mathematics and Theoretical Physics, Centre for Mathematical Sciences, University of Cambridge, Wilberforce Road, Cambridge CB3 0WA, United Kingdom

In this paper, we present results for large-angle cosmic microwave background anisotropies generated from high resolution simulations of cosmic string networks in a range of flat Friedmann-Robertson-Walker universes with a cosmological constant. Using an ensemble of all-sky maps, we compare with the Cosmic Background Explorer data to infer a normalization (or upper bound) on the string linear energy density μ. For a flat matter-dominated model ($\Omega_M = 1$) we find $G\mu/c^2 \approx 0.7 \times 10^{-6}$, which is lower than previous constraints probably because of the more accurate inclusion of string small-scale structure. For a cosmological constant within an observationally acceptable range, we find a relatively weak dependence with $G\mu/c^2$ less than 10% higher.

I. INTRODUCTION

Given the growing evidence for a cosmological constant or dark energy component in the Universe, it is important to determine whether or not this significantly impacts the evolution of cosmic strings and their observational signatures. The strongest constraint limiting the energy scale of cosmic strings is currently the Cosmic Background Explorer (COBE) normalization of large-angle cosmic microwave background (CMB) anisotropy. In this paper, we will infer this normalization from maps computed using the methods presented in [1] and determine how this is influenced by late-time domination by a cosmological constant.

II. METHOD

A. Geometry of simulations

To compute all-sky maps, the "observers" are located inside the simulation box. Following [2], we place eight such observers at each corner of a cube of side $L/2$ where L is the size of the box itself. We use the fact that the string networks, and hence the cosmological perturbations they induce, have periodic boundary conditions to identify opposite sides of the box. The eight realizations of the sky are not completely independent, but the correlations are not apparent. This scheme reduces the effect of the cosmic variance on large angular scales and thus renders the computation of the normalization more accurate.

B. Pixelization

To facilitate the computation of maps and the extraction of the power spectrum, we use an iso-latitude pixelization,

which enables us to Fourier transform each ring of constant θ to evaluate the integral over the azimuthal angle. More specifically, we use the equal area with 3:6:3 base pixels, proposed by [3]. In this scheme, each base pixel is subdivided into $n^2 = 2^{2p}$ pixels. The area of a pixel is given by $A_{pixel} = 4\pi/N_{pixel} = \pi/3n^2$. But, by integrating the spherical surface element over a pixel, we have $A_{pixel} = (2\pi/N_p)\Delta\cos\theta$. Hence, the width of a row of pixels is given by

$$\Delta\cos\theta = \frac{N_p}{6n^2}, \tag{1}$$

where N_p is the number of pixels per row of constant θ. In the polar caps, $N_p = 3$, then $9 \times 2^{i-2}$ repeated 2^{i-2} times with $2 \leq i \leq p+2$. The equatorial regions are made up of n rows of $6n$ pixels.

C. Angular power spectrum computations

The pixelized map is the convolution of the real temperature map with the pixel window function. To compute the power spectrum, we need to know the spherical transform of the window function. In real space, the pixel window function is simply given by

$$W^{pq}(\phi, \theta) = \begin{cases} \dfrac{1}{A_{pixel}} & \text{inside the pixel,} \\ 0 & \text{outside,} \end{cases} \tag{2}$$
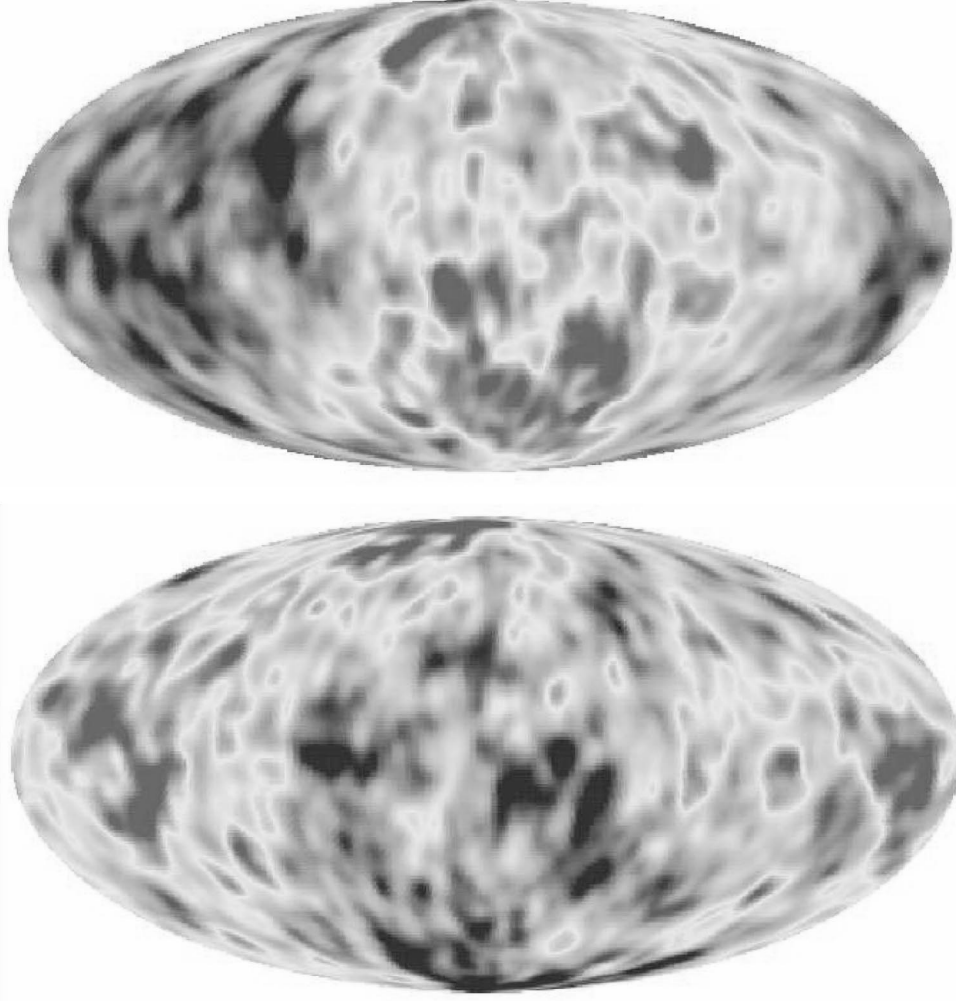
where p and q label the rows and the pixels on that row:

$$T^{pq} = \int_{S_2} T(\phi, \theta) W^{pq}(\phi, \theta) d\Omega = \sum_{m=-\ell_{max}}^{\ell_{max}} b_m e^{imq2\pi/N_p}, \tag{3}$$

where

*Electronic address: landriau@lal.in2p3.fr

[†]Electronic address: E.P.S.Shellard@damtp.cam.ac.uk

FIG. 1. All-sky string-induced maps for a flat FRW Universe with $\Omega_\Lambda = 0$ and 0.7.

$$b_m = \sum_{\ell=|m|}^{\ell_{max}} a_{\ell m} w(\pi m/N_p)\bar{\lambda}_\ell^m, \qquad (4)$$

with

$$w(\psi) = e^{i\psi}\frac{\sin\psi}{\psi}$$

$$\overline{\lambda_\ell^m} = \frac{1}{\cos\theta_p - \cos\theta_{p+1}}\int_{\cos\theta_p}^{\cos\theta_{p+1}} \lambda_\ell^m(\cos\theta)d(\cos\theta). \quad (5)$$

From the last line in Eq. (3), the b_m can be obtained by the inverse sum:

$$b_m = \sum_q T_{pq} e^{-imq2\pi/N_p}, \qquad (6)$$

which can be done using a fast Fourier transform. Sum (4) can also be inverted to obtain the $a_{\ell m}$'s:

$$a_{\ell m} = \frac{\displaystyle\sum_{p=1}^{n_{rows}} b_m w^*(\pi m/N_p)\overline{\lambda_\ell^m}}{\displaystyle\sum_{p=1}^{n_{rows}} w^*(\pi m/N_p)w(\pi m/N_p)N_p}. \qquad (7)$$

To obtain this last equation, we took the approximation that the pixelized spherical harmonics $w(\pi m/N_p)\overline{\lambda_\ell^m}$ are orthogonal, which is valid at low ℓ.

D. COBE normalization

To infer the cosmic string linear energy density, we use the COBE angular correlation function because, on the scales of interest, it is as good as that of the Wilkinson Microwave Anisotropy Probe [4]. This also enables direct comparisons with previous work.

To normalize to COBE, we follow [5] and compute the angular correlation function using

$$C(\theta,\theta_s) = \frac{1}{4\pi}\sum_\ell (2\ell+1)|W_\ell|^2|B_\ell|^2 C_\ell P_\ell(\cos\theta), \quad (8)$$
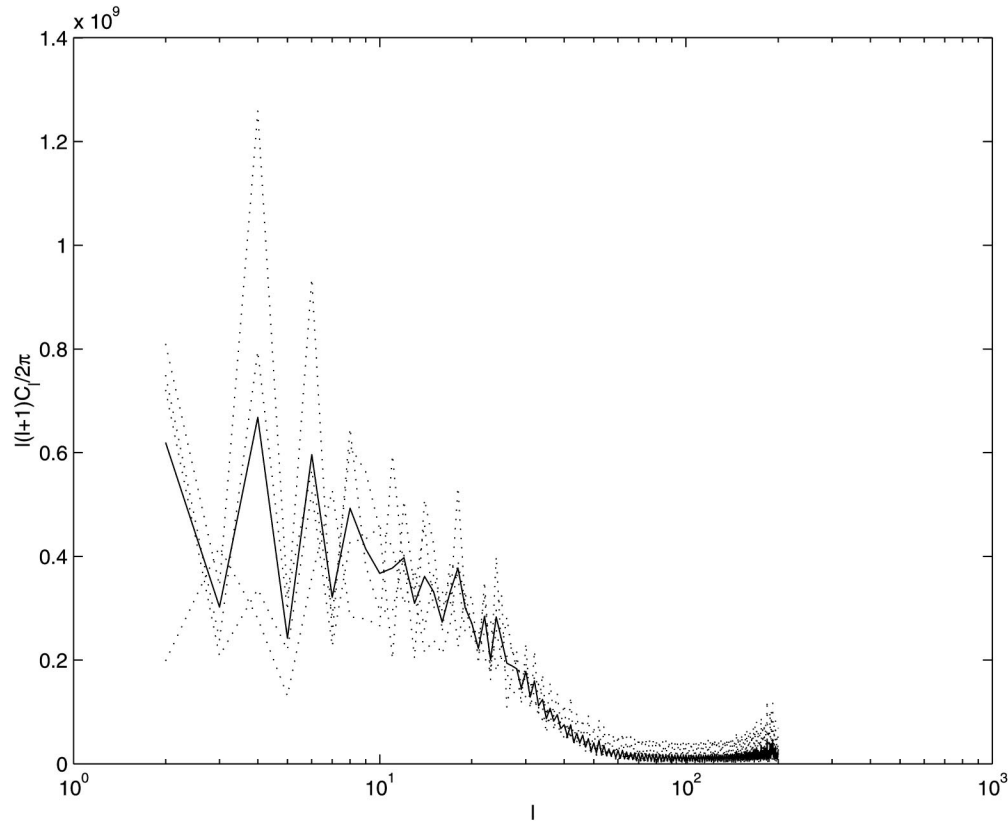
FIG. 2. Individual power spectra for the $\Omega_\Lambda=0$ run (dotted) with the average (solid).

where we use the following smoothing function:

$$W_\ell(\theta) = \exp\left(-\frac{\ell(\ell+1)}{\log 2}\sin^2(\theta/4)\right), \qquad (9)$$

where θ is the smoothing scale. We also use the COBE beam profile B_ℓ given in [6]. We then compare the result with the value obtained by the 4 year COBE maps [7], $C(0°,10°) = (29\pm1 \ \mu K/T)^2$ to infer the value of $G\mu/c^2$. In the previous equation, T is the mean temperature of the CMB also obtained from COBE [8] $T=2.726\pm0.002$ K.

III. RESULTS

A. Cosmic string simulations

We created a time series of cosmic string realizations using the Allen-Shellard network simulation [9] in a variety of flat Friedmann-Robertson-Walker (FRW) universes with $\Omega_m+\Omega_\Lambda=1$, where Ω_m includes the contribution of dark matter and baryons. These string networks were then used as sources for the CMB map-making pipeline. For all the simulations, we chose $h=0.72$ and $\Omega_b h^2=0.02$.

Two string simulations for $\Omega_\Lambda=0$ and $\Omega_\Lambda=0.7$ were computed with very high resolution with over 3×10^6 points (16 points per correlation length) and spanning a dynamic range of 5 in conformal time, probing the Universe back to $z=25$ and $z=30$, respectively. All string loops were retained in the simulation to ensure overall network energy-

momentum conservation, which was preserved at the level of 1%. Point joining was used only to ensure a consistent physical resolution, i.e. removing very short segments formed through reconnection. The simulations therefore retained their full small-scale structure. These were the costliest part of the pipeline and took many days to perform on the COS-MOS supercomputer (≈2000 h of CPU time). This improves upon previous work with string networks in an expanding Universe, which was performed with fewer points per correlation length, fixed horizon resolution and a separate treatment of loops [5,10].

In addition, we performed a series of smaller simulations (10^6 points) for different values of the cosmological constants, specifically, $\Omega_\Lambda=0, 0.2, 0.4, 0.55, 0.7, 0.85$. These simulations had identical initial conditions, so comparisons could minimize the effects of cosmic variance.

The map-making pipeline was tested at resolutions of 128^3 and 256^3. The huge data storage requirements with string networks, scalar-vector-tensor- (SVT-) decomposed energy-momentum tensor grids, Boltzmann code output plus checkpointing files meant disk space approaching 1 Tbyte was required for 256^3. Further parallelization issues remain to be resolved for large memory runs.

In Fig. 1, we present realizations for the $\Omega_\Lambda=0$ and 0.7 runs. The angular power spectra for each of these runs are presented in Fig. 3. We also show four spectra obtained from the $\Omega_\Lambda=0$ run with their average in Fig. 2. All these spectra are normalized to COBE.
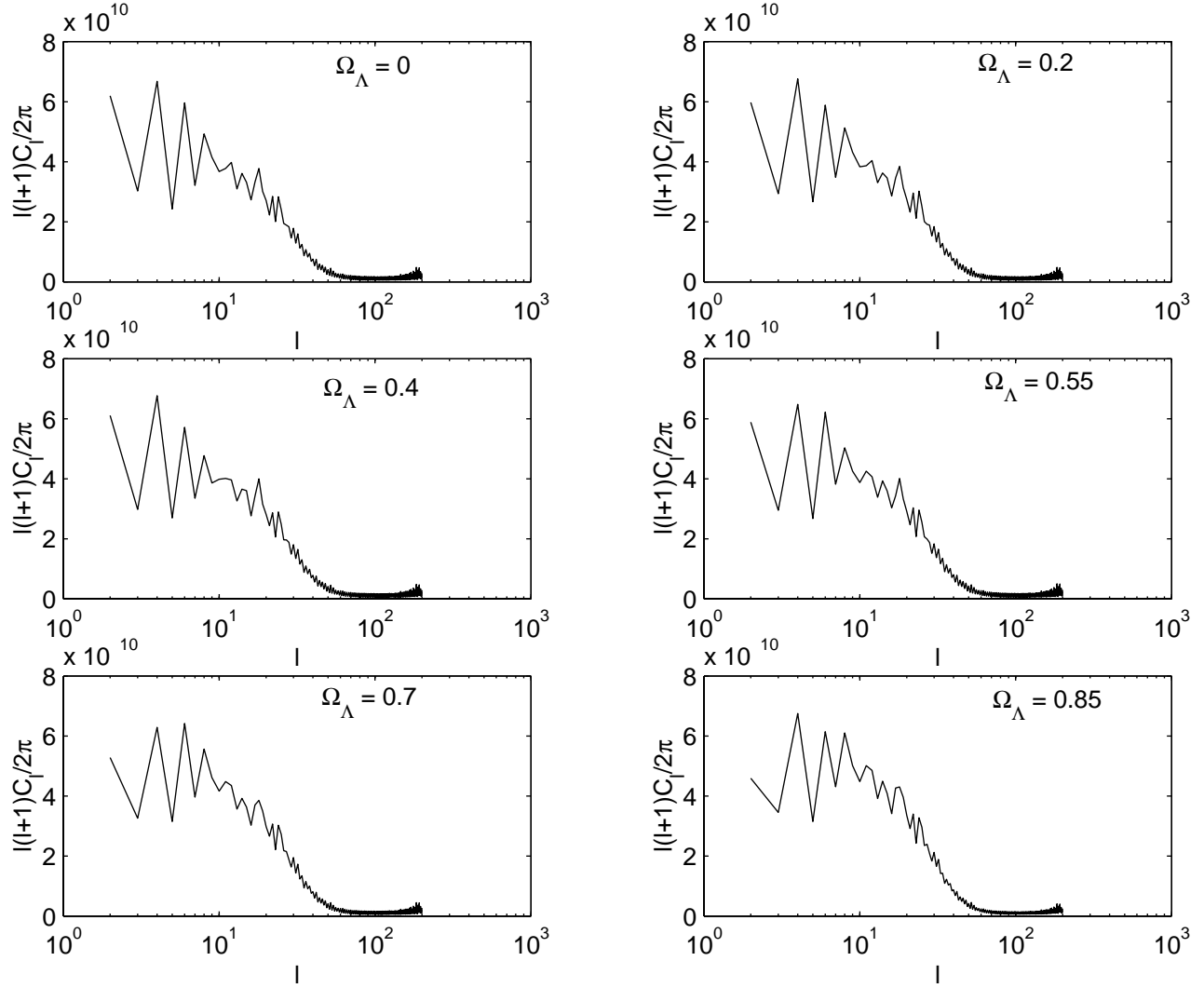
FIG. 3. Average power spectra for each run.

B. Normalization to COBE

The power spectra illustrated in Figs. 2 and 3 show a roughly scale invariant plateau for $\ell \lesssim 20$ with a gradual fall-off to an insignificant signal beyond $\ell \gtrsim 50$. This falloff is a consequence of the limited dynamic range of the string simulations and not of the resolution at which the Boltzmann evolution was performed (though there is some influence from the interpolation and smoothing of the string network onto the grids.

Previous CMB work with string networks over a much larger dynamic range has demonstrated that the main anisotropies relevant to COBE are generated at redshifts $z \lesssim 20$ [5], which is within the range of the present work. The reason for this can be seen from studies of the unequal-time correlators [11,12], which peak on scales well below the horizon ($\lambda_{max} < d_H/3$). We are confident therefore that our simulations include the primary contributions on COBE scales.

This scale invariance on large angular scales is consistent with the COBE data and allows us to normalize our results accordingly, as discussed above, providing a constraint on the energy density of strings. Our normalization for the flat cold dark matter (CDM) model,

$$\frac{G\mu}{c^2} = (0.7 \pm 0.2) \times 10^{-6}, \tag{10}$$

has an error reflecting the variance of our results, not systematic effects which may be comparable. This result is lower but consistent with the previous result [5]:

$$\frac{G\mu}{c^2} = (1.05^{+0.35}_{-0.2}) \times 10^{-6}. \tag{11}$$

Our result is significantly lower than that obtained in [10], $G\mu/c^2 = 1.7 \times 10^{-6}$ from a single simulation. This work however focused on small angle anisotropies and did not study sample variance at large angles. Other flat space approximations and semi-analytic estimates for local string networks generally have found a higher normalization than ours, e.g. $G\mu/c^2 = (1.5 \pm 0.5) \times 10^{-6}$ [13], $G\mu/c^2 = (1.7 \pm 0.7) \times 10^{-6}$ [14] and $G\mu/c^2 = 2$ [15].
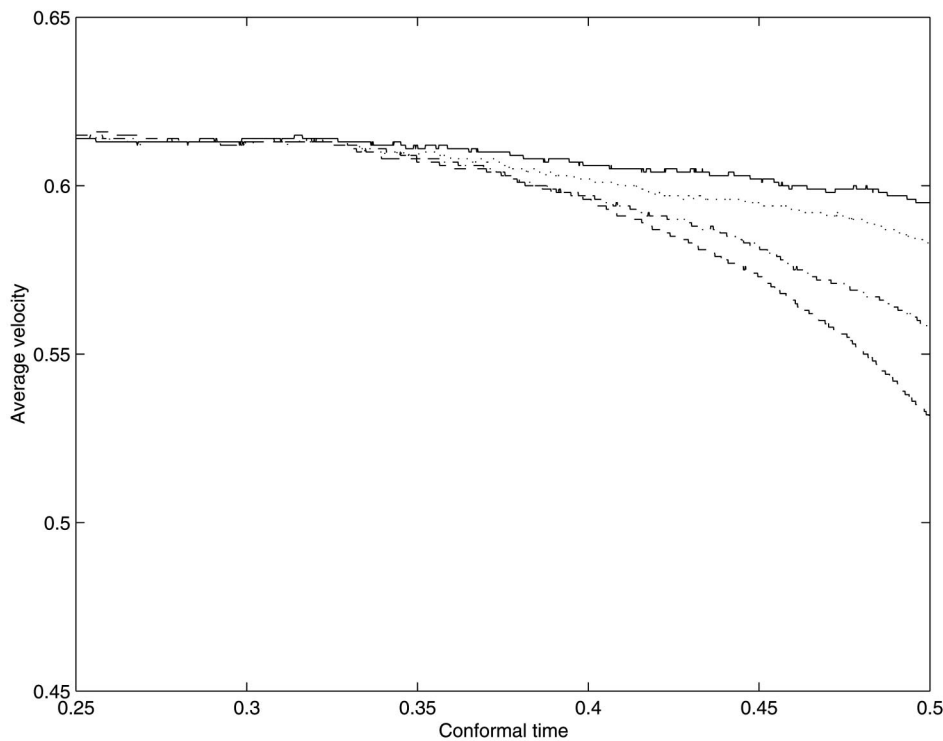
FIG. 4. Average rms long string velocity for the last half of the string network simulations for $\Omega_\Lambda = 0$ (solid), $\Omega_\Lambda = 0.4$ (dotted), $\Omega_\Lambda = 0.7$ (dot-dashed) and $\Omega_\Lambda = 0.85$ (dashed). Even the extremal Λ model shows only a relatively small 11% decline in the average string velocity by the present day. (Relative conformal time is plotted with $\eta_0 = 0.5$.)

However, there is a key reason why the present work is a significant advance over these previous analyses. Apart from now including all the relevant physics, this analysis uses the highest resolution string simulations to date. The initial points per correlation length have been chosen at levels known to preserve small scale structure accurately [16] and

the simulations are evolved at fixed physical resolution. Although the simulations used in [5] spanned a larger dynamic range, $z < 100$ (compared to our $z < 25$), it did so by maintaining fixed horizon resolution through point joining and smoothing. Subsequent work has shown that at least comoving resolution is required if we are to hope for a satisfactory
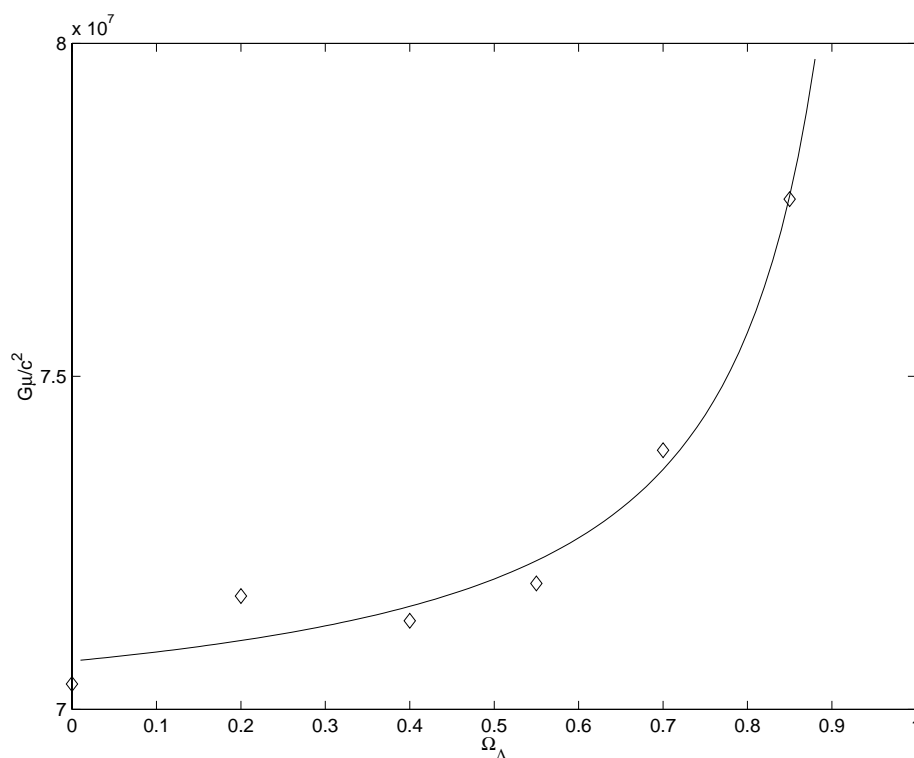

FIG. 5. String linear energy density obtained from the COBE normalization. The solid line is curve (12).

treatment of string wiggliness. This implies that the previous work did not adequately account for the renormalized string energy per unit length, which in the matter era is $\tilde{\mu} \simeq 1.4\mu$. Such a factor would tend to increase the string anisotropy, thus lowering the COBE normalization of $G\mu/c^2$ (though in a non-trivial manner).

C. Effect of the cosmological constant

The influence of Ω_Λ on the COBE normalization, illustrated in Fig. 5 is relatively small: for the popular value of $\Omega_\Lambda = 0.7$ we obtained $G\mu/c^2 = (0.74 \pm 0.20) \times 10^{-6}$, only 6% higher than for the flat CDM model.

The reason for the reduced anisotropy in Λ models is fairly clear. As the Universe becomes vacuum dominated at late times, the expansion rate increases, affecting the Hubble damping term $\dot{a}/a$ in the string equations of motion, thus lowering their average velocity as can be seen from Fig. 4. As string velocities are the primary cause of CMB anisotropies, there will be a net reduction in $\Delta T/T$.

The smallness of this effect is somewhat surprising, but is explained by the late redshift of vacuum domination. In the $\Omega_\Lambda = 0.7$, this occurs at $z_\Lambda \simeq 0.33$, which, in the context of our simulations, implies that Λ has a significant effect on only the later stages of the simulation. Comparing the $\Omega_\Lambda = 0.85$ model with the flat CDM model in Fig. 3, there appears to be a slight relative falloff in the average power towards $\ell = 2$, which is consistent with this picture. However, this effect is likely to be swamped by cosmic variance.

We have found that our data points are well fitted by

$$\frac{G\mu}{c^2} = \left(0.695 + \frac{0.012}{1 - \Omega_\Lambda} \right) \times 10^{-6}. \qquad (12)$$

This analytic fit is motivated by the asymptotic limit in which string velocities should vanish as the network is frozen and conformally stretched in an extreme Λ model: $\Omega_\Lambda \rightarrow 1$ and $\Omega_m \rightarrow 0$. Our results are summarized in Table I and plotted in Fig. 5 along with fit (12).

IV. SUMMARY

In this paper, we presented large angle maps of CMB fluctuations seeded by networks of cosmic strings in flat FRW universes with a cosmological constant. From the

TABLE I. String linear energy density obtained from the COBE normalization.

Ω_Λ	$G\mu/c^2 \times 10^{-6}$
0.00	0.7038 ± 0.1947
0.20	0.7170 ± 0.1926
0.40	0.7133 ± 0.1989
0.55	0.7189 ± 0.1902
0.70	0.7389 ± 0.1990
0.85	0.7766 ± 0.1879

COBE data, we have obtained a constraint on the string linear energy density $G\mu/c^2 \lesssim 0.7 \times 10^{-6}$ which is lower than previous work because string small-scale structure is incorporated more accurately in the network simulations. We were able to find the dependence of the string density μ as a function of the cosmological constant, obtaining a good fit with a simple semi-analytic formula. Given the uncertainties in the overall normalization, these results should provide an adequate means by which to characterize the effects of Ω_Λ on cosmic string models.

Although current CMB data have shown that cosmic strings cannot be the dominating source of CMB anisotropies (e.g., Ref. [17]), they can nonetheless be present albeit at a lower energy scale. For example, they are copiously produced at the end of brane inflation [18,19]. With this in mind, our normalization appears low when compared with the value inferred from the possible detection of a gravitational lensing event by a cosmic string: $G\mu/c^2 \approx 0.4 \times 10^{-6}$ [20]. This linear mass density would be somewhat higher than allowed in the standard cosmic string scenario considered in this paper.

[1] M. Landriau and E.P.S. Shellard, Phys. Rev. D **67**, 103512 (2003).
[2] U.L. Pen, D.N. Spergel, and N. Turok, Phys. Rev. D **49**, 692 (1994).
[3] R.G. Crittenden and N.G. Turok, astro-ph/9806374.
[4] M. Halpern (private communication).
[5] B. Allen, R.R. Caldwell, E.P.S. Shellard, A. Stebbins, and S. Veeraraghavan, Phys. Rev. Lett. **77**, 3061 (1996).
[6] E.L. Wright *et al.*, Astrophys. J. **420**, 1 (1994).
[7] A.J. Banday *et al.*, Astrophys. J. **475**, 393 (1997).
[8] C.L. Bennett *et al.*, Astrophys. J. Lett. **464**, L1 (1996).
[9] B. Allen and E.P.S. Shellard, Phys. Rev. Lett. **64**, 119 (1990).
[10] B. Allen, R.R. Caldwell, S. Dodelson, L. Knox, E.P.S. Shellard, and A. Stebbins, Phys. Rev. Lett. **79**, 2624 (1997).
[11] A. Albrecht, D. Coulson, P.G. Ferreira, and J. Magueijo, Phys. Rev. Lett. **76**, 1413 (1996).
[12] J.H.P. Wu, P.P. Avelino, E.P.S. Shellard, and B. Allen, Int. J. Mod. Phys. D **11**, 61 (2002).
[13] D.P. Bennett, A. Stebbins, and F.R. Bouchet, Astrophys. J. Lett. **399**, L5 (1992).

[14] L. Perivolaropoulos, Phys. Lett. B **298**, 305 (1993).

[15] D. Coulson, P. Ferreira, P. Graham, and N. Turok, Nature (London) **368**, 27 (1994).

[16] C.J.A.P. Martins and E.P.S. Shellard (unpublished).

[17] C.L. Bennett *et al.*, Astrophys. J., Suppl. Ser. **148**, 1 (2003).

[18] S. Sarangi and S.H.H. Tye, Phys. Lett. B **536**, 185 (2002).

[19] L. Pogosian, S.H.H. Tye, I. Wasserman, and M. Wyman, Phys. Rev. D **68**, 023506 (2003).

[20] M. Sazhin *et al.*, Mon. Not. R. Astron. Soc. **343**, 353 (2003).